Science Bulletin 64 (2019) 1310–1317

Contents lists available at ScienceDirect

Science Bulletin

journal homepage: www.elsevier.com/locate/scib

Article

Crystal structure of a bacterial homolog to human lysosomal transporter, spinster

Fu Zhou [a,1], Deqiang Yao [b,2,1], Bing Rao [a], Li Zhang [a], Wang Nie [c], Yan Zou [c], Jie Zhao [d,*], Yu Cao [b,d,*]

[a] CAS Center for Excellence on Molecular Cell Science, Institute of Biochemistry and Cell Biology, Chinese Academy of Sciences, University of Chinese Academy of Sciences, Shanghai 201210, China
[b] Institute of Precision Medicine, The Ninth People's Hospital, Shanghai Jiao Tong University School of Medicine, Shanghai 200125, China
[c] School of Life Science and Technology, ShanghaiTech University, Shanghai 201210, China
[d] Department of Orthopaedics, Shanghai Key Laboratory of Orthopaedic Implant, Shanghai Ninth People's Hospital, Shanghai Jiao Tong University School of Medicine, Shanghai 200011, China

ARTICLE INFO

Article history:
Received 10 June 2019
Received in revised form 10 July 2019
Accepted 17 July 2019
Available online 12 August 2019

Keywords:
Major facilitator superfamily
Transporter
Spinster
Membrane protein

ABSTRACT

Lysosomes break down various biomolecules and spinster is one of the major efflux carriers removing degradation products from lysosomal lumen to keep it in healthy size and proper function. Although it is well established that a dysfunctional spinster will cause enlarged lysosomes and in turn lead to developmental defects and abnormal behavior in animals, little was known about the transportation mechanism and substrate specificity of spinster. Here, we report a crystal structure of spinster homolog from Hyphomonas neptunium, HnSPNS, in its inward-facing conformation with and without substrate bound. HnSPNS is crystallized in a monomer and a substrate-binding cavity was formed in the center of its transmembrane helices. A blob of electron density corresponding to its substrate was found in the cavity near a conserved residue, R42, which is locked in position by the interactions with conserved residues E129 and R122. Our results suggest that human spinster serves as a transporter translocating negatively-charged lipophilic small molecules and E129 might serve as a switch to control the conformational change via its protonation-deprotonation cycle.

1. Introduction

The lysosomal efflux transporter, spinster (SPNS), plays a central role in cellular senescence by maintaining the lysosome morphology and regulating autolysosomes formation. As a class of multi-pass membrane proteins conserved among the species from insect to human, the spinster was predicted as transporter family with functions largely associated to the small molecules exchange of lysosomes and bioactive lipids permeation through the cell membrane. The animals with SPNS gene mutations or knockout showed enlarged lysosomes and late endosomes, in turn resulting in abnormal synaptic growth and neurodegeneration [1–3]. The SPNS gene was first identified in drosophila and the loss-of-function mutation of SPNS results in rejection behaviors of female in mating activities, along with abnormal development in the reproductive system and enlarged synapse [2–4]. The associations between developmental errors and spinster gene mutation were also observed in other organs and tissues and the consequences of dysfunctional spinster include glia over-migration into eye imaginal discs [5], disruption on heart tube and the formation of dual-heart structure [6], ectopic cartilage and jaw reductions [7], and modification on lymphocyte composition [8].

SPNS is a subfamily of major facilitator superfamily (MFS) and extensively found in most eukaryotic cells, with some homologs found in bacterial genus of *Geobacter*, *Sphingomonas*, and *Hyphomonas*, etc., having an amino acid sequence identity ranging from about 20% to 35% to human spinster protein. There are three SPNS family members in human (hsSPNS1-3) and four members in nematode (ceSPNS1-4) sharing sequence identities of 28%–40% with drosophila spinster protein. SPNS1 (or *benchwarmer* in drosophila and *not really started* in zebrafish) was mostly found in lysosomal membrane and predicted as a potential sugar transporter according to its amino acid sequence while cell biology study on npc (−/−) mice, an animal model of Niemann-Pick type C disease (NPC), implied the role of SPNS1 in leucine export from lysosomes [9]. The impaired SPNS1 func-

* Corresponding authors.
E-mail addresses: 13301815365@189.cn (J. Zhao), yu.cao@shsmu.edu.cn (Y. Cao).
[1] These authors contributed equally to this work.
[2] iHuman Institute, ShanghaiTech University, Shanghai 201210, China (present affiliation for D.Y.).

https://doi.org/10.1016/j.scib.2019.08.010
2095-9273/

tion might result in the over-storage of carbohydrates and lipids in lysosomes [2,3,10], in turn leading to a defected endocytosis pathway and protein degradation in lysosomes and accumulation of autolysosomes [11,12], which makes SPNS1 deficiency animal a promising model for lysosomal storage disease (LSD). SPNS2, a close relative to SPNS1, was mostly found in cytoplasmic membrane and showed sphingosine-1-phosphate (S1P) transportation activity, in turn regulating the signaling pathway by activating S1P receptors [13]. The S1P secretion through SPNS2 plays a critical role in controlling S1P level in circulatory fluids and thus boosts the function of immune cells in lymph, such as natural killer cells [14] and naive T cells [15], implying that SPNS2 might be a potential immunosuppressant drug target [16,17].

The most mysterious part about spinster proteins is their substrate specificity and transportation mechanism. Although it was widely proposed that SPNS1 and 2 could recognize and catalyze the cross-membrane permeation of sugars and S1P, respectively, most evidence for their biochemical functions were built on the abnormal accumulation of putative substrate in SPNS-deficient animal or cell-based measurement. A structural model for spinster protein will help understand how SPNS binds to its cargo molecules and the mechanism underlying the disorder resulting from its gene mutation. To answer those questions, we attempted to determine the structure for SPNS protein and its homologs and after failure to purify functional protein of eukaryotic SPNS, we solved the crystal structure for the bacterial ortholog of spinster protein from Hyphomonas neptunium at 3.1 Å, and identify the substrate recognition region, as well as the critical residues in a putative substrate binding. The highly conserved binding pocket for substrate was analyzed for its chemical properties which align well with the requirement for capturing a lipophilic and negative charged molecule, e.g., S1P.

2. Materials and methods

2.1. Cloning and purification of HnSPNS protein.

The HnSPNS gene (Uniprot ID Q0C3L8) was amplified from Hyphomonas neptunium genomic DNA and cloned into a plasmid modified from pET vector with a C-terminal flag tag a TEV protease recognition site with a kanamycin-resistance gene. The expression plasmid was transformed into *E. coli* Rosetta (DE3) strain and the overexpression for native protein was induced by adding isopropyl-β-D-thiogalactoside (IPTG) to a final concentration of 0.2 mmol/L after cell culture reached the density of O.D. 600 nm 1.0 in Luria broth; for expression of selenomethionine (SeMet)-incorporated proteins, the cells were grown in minimal medium containing 32.2 mmol/L K_2HPO_4, 11.7 mmol/L KH_2PO_4, 6 mmol/L $(NH_4)_2SO_4$, 0.68 mmol/L Na citrate, 0.17 mmol/L Mg_2SO_4, 32 mmol/L glucose, 0.008% (w/v) alanine, arginine, aspartic acid, asparagine, cysteine, glutamic acid, glycine, histidine, proline, serine, tryptophan, glutamine and tyrosine, 0.02% (w/v) isoleucine, leucine, lysine, phenylalanine, threonine and valine, 25 mg/L L-selenium-methionine, 32 mg/L thiamine, and 32 mg/L thymine, to O.D.600 nm 0.6 before induction with IPTG. The cell was further grown at 20 °C for 12–14 h and harvested by centrifugation. The cell membranes were solubilized with 40 mmol/L *n*-decyl-β-D-maltoside (Anatrace) and the Flag-tagged protein was purified with ANTI-FLAG M2 Resin (SIGMA). After removal of the tag with tobacco etch virus protease, the native protein was subjected to size-exclusion chromatography with a Superdex 200 Increase 10/300 GL column (GE Health Sciences) equilibrated in 150 mmol/L NaCl, 20 mmol/L HEPES, pH 7.5 and 4 mmol/L *n*-decyl-β-D-maltoside. The SeMet-incorporated HnSPNS protein was purified by the same procedure. Fractions of the peak are pooled and the purity of was estimated with SDS-PAGE.

2.2. Crystallization

Purified HnSPNS protein was concentrated to about 15 mg/mL and mixed in sitting drops at 4 °C with equal volume of crystallization solution. The native crystals were grown using crystallization solution comprising 32.5% (v/v) polyethylene glycol 400, 100 mmol/L Tris-HCl, pH 7.4 by vapor diffusion and harvested in 3–5 days by directly flash freezing into liquid nitrogen. The SeMet-incorporated crystals were grown in crystallization solution comprising 25% polyethylene glycol 600, 100 mmol/L HEPES, pH = 7.5 by micro-seeding method using pre-formed native HnSPNS crystal nuclei and flash frozen into liquid nitrogen after cryo-protected in crystallization solution supplemented with 10% glycerol for 2–5 s.

2.3. Data collection and structure determination

Diffraction data were collected at the Shanghai Synchrotron Radiation Facility (SSRF) beamlines BL18U1 for native crystal and BL19U1 for the SeMet-incorporated crystal. The data were collected and processed with XDS [18]. Two datasets from two SeMet-incorporated crystals were merged to improve anomalous signal for experimental phasing. The crystallographic parameters and data collection statistics are given in Table S1 (online). The structure was solved by Se-SAD method. The sites of Se were determined with program of SHELXD [19]. Phasing and initial model building were performed in Phenix [20]. Iterative cycles of refinement were carried out using PHENIX, Refmac5 [21,22] and Coot [23].

3. Results

3.1. Spinster overall structure

While the recombinant expression of SPNS proteins from eukaryotes such as human, mouse, and drosophila was unsuccessful, a SPNS-like protein from *H. neptunium*, named as HnSPNS hereafter, was expressed in *E. coli* and purified with good stability and purity as determined by SDS-PAGE and gel filtration. HnSPNS shares sequence identities of 22% and 18% with human SPNS1 and SPNS2, respectively (Fig. S1 online). The full-length HnSPNS was crystallized in several detergents, e.g., *n*-Dodecyl β-D-Maltoside (DDM), *n*-Decyl β-D-Maltoside (DM) and *n*-Nonyl β-D-Maltoside (NM), and the crystal in DM diffracts to about 3.2 Å allowing the structural determination. The crystal is of space group $P2_12_12_1$ and contains a single HnSPNS molecule in each asymmetric unit. As shown in Fig. 1a, the Transmembrane domain of HnSPNS consists of 12 transmembrane α-helices (H1−12), connected with loops and 6 short helices (HA – HE for extracellular helices and HI for intracellular helix). Similar to other MFS transporter like GlpT [24], LacY [25] and FucP [26], HnSPNS has its 12 TM helices assemble two structural repeats with pseudosymmetry: N repeat and C repeat are comprised of H1-6 and H7-12, respectively (Fig. 1d), with an interface built with the 2nd and 5th helices of each repeat, i.e., the H2–H11 pair and H5–H8 pair (Fig. 1c, d); and the MFS signature sequences DRXXRR [27] was found at H2-H3 linker but missed in C-repeat of HnSPNS. The N- and C-repeats are connected with a long and flexible loop, the "hinge loop", which was solved with SeMet hnSPNS crystal with low-quality electron density and absent in native crystal structure, implying a dynamic nature for this region in transporter function. The helices H3/H6/H9/H12 are arranged distally at sides and not

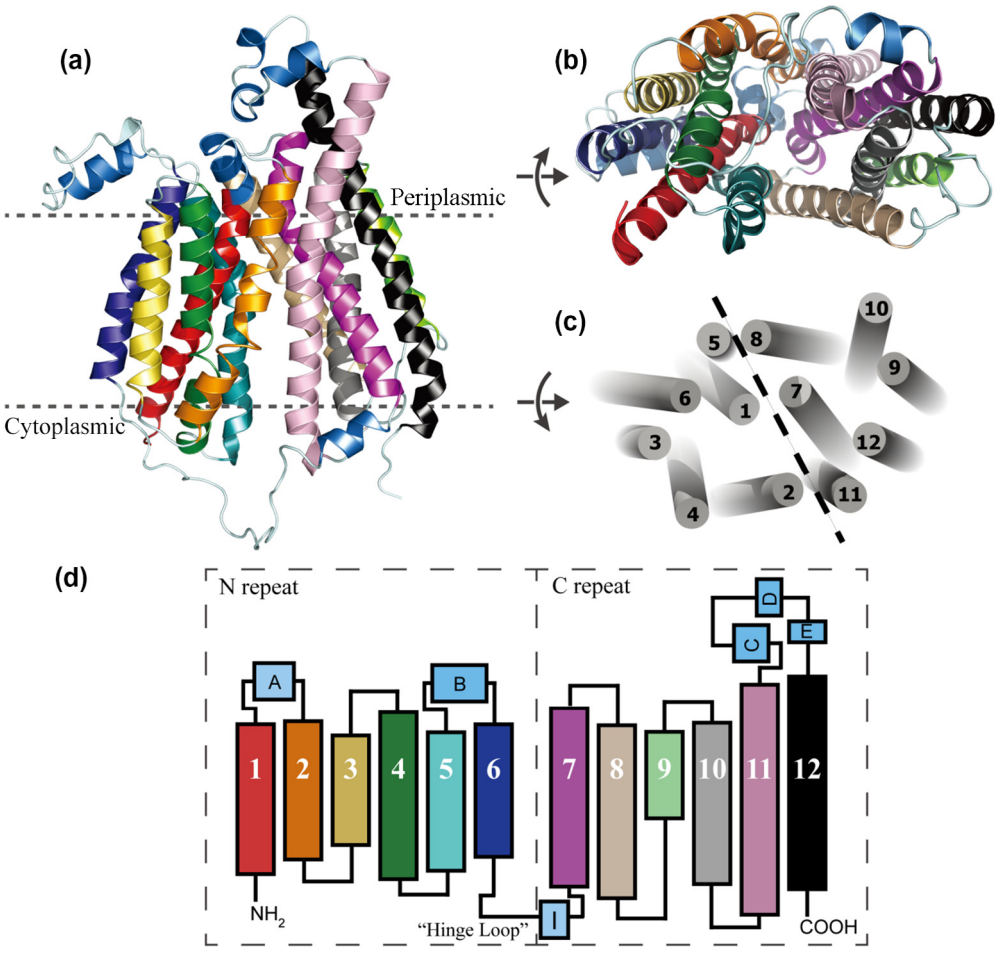

Fig. 1. Overall architecture of HnSPNS. (a) The HnSPNS colored by transmembrane helices and viewed parallel to the membrane. The cell membrane was shown with dotted line and the orientation labeled according to the calculation using PPM server (https://opm.phar.umich.edu/ppm_server). (b) HnSPNS viewed from the intracellular side. The monomeric HnSPNS is rotated by 90° about x axis related to the model in (a). (c) Top view of HnSPNS. The monomeric HnSPNS was sliced along the extracellular surface of membrane to show the TM helices organization with its extracellular helices and loops removed for a clear observation. Each TM helices was numbered in order from N- to C-terminal of protein. (d) Cartoon representation of HnSPNS topology. The TM helices H1-12, extracellular helices HA-HE and intracellular helix HI were colored according to the same scheme as in (a) and (b). Please note all structure graphs in this paper were produced using PyMOL (The PyMOL Molecular Graphics System, Version 1.9 Schrödinger, LLC.).

involved in the central core of spinster. The HnSPNS molecule was crystallized in an inward-open conformation (C_i) and adopts a bell-shape when viewed parallel to the membrane, with a wide mouth open to cytoplasmic space and a constricted crown at the extracellular side.

3.2. The inner cavity and conserved domain

HnSPNS adopts a typical MFS-fold and in each protomer exists an inner cavity sandwiched by its N- and C-repeat as shown in Fig. 2a, which might represent the substrate translocation cavity. The SPNS cavity forms a rough pyramid shape with an approximate volume of 7540 $Å^3$ calculated by the method developed by Voss et al. [28] and the opening at the cytoplasmic side measures about 10 Å × 26 Å. In comparison with other known structures of transporters in their inward-open conformation, the SPNS cavity is smaller than that of LacY (10,684 $Å^3$) but larger than the cavities in GlpT (7,295 $Å^3$) and NarU (5,321 $Å^3$). Interior spaces analysis on HnSPNS shows an overall hydrophobic surface with some charge-rich regions, especially the portion near to N-repeat largely carrying positive charges (Fig. 2a). More than 50% of the residues conserved among spinster protein from various species are localized around the inner cavity and furthermore, most of them (14 out of 18) are found in N-repeat of HnSPNS (Fig. 2a, left and right panel). Compared with solute transporters shown in Fig. 2b, HnSPNS has a cavity with fewer charges and hydrophilicity, implying a lipidic or lipophilic nature for its transportation substrates.

SPNS genes maintain moderate sequence conservation during evolution and share 20%–35% sequence identity among species from bacteria to mammals Fig. S1 (online). Most of conserved residues gather in three structural loci within N-repeat of SPNS (Fig. 3a), which form contacts between H2 and H4 in the inner cavity (Fig. 3b), between H1 and H4 near to extraplasmic surface (Fig. 3c), as well as an interlocking among H2, H4, H5, and the loop linking N- and C-repeats, near to intracellular surface (Fig. 3d). The conserved region in the inner cavity contains two well-characterized residues in spinster functional studies, E129 and R122, and the mutations on their equivalent residues, E217 in drosophila and R153 in zebrafish, respectively, could abolish the transportation function [1,11,13]. As shown in Fig. 3c, E129 and R122 form salt bridges with the ε-nitrogen and carboxyl oxygen of R42, respectively, which stabilize the α-helices bundle within membrane and imply the importance of R42 in the structural integrity and function of spinster protein. A "DRXXRX" motif con-

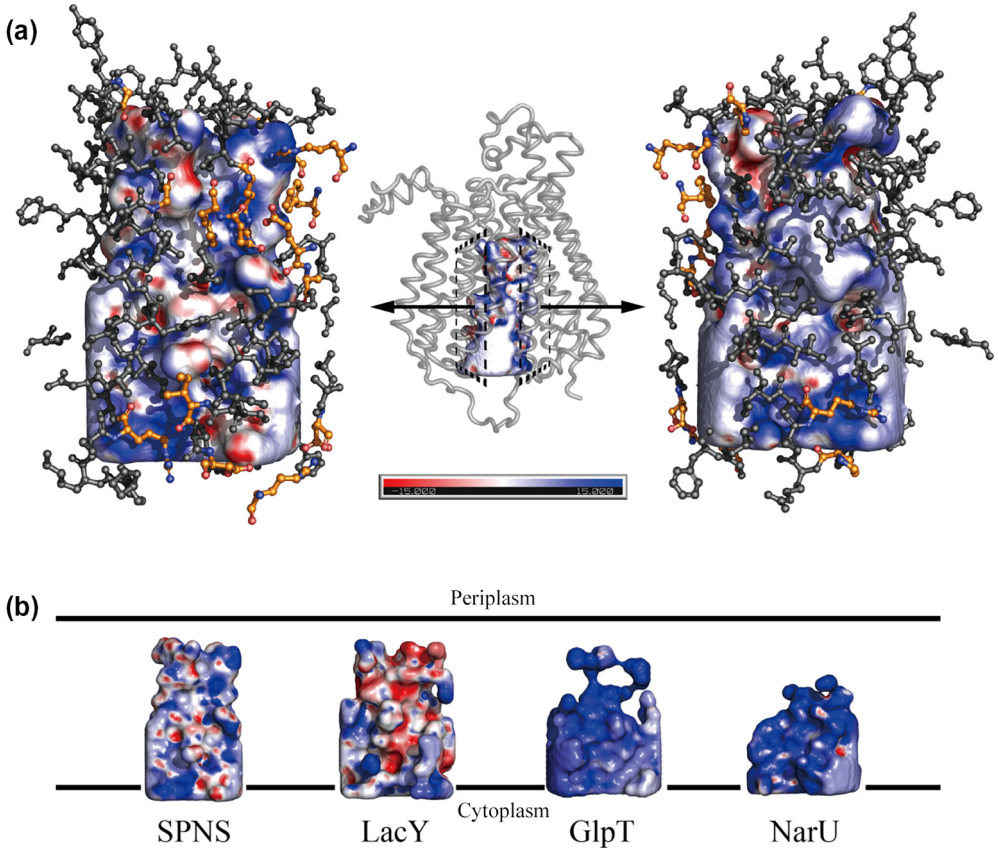

Fig. 2. The central cavity and conserved residue in hnSPNS. (a). Middle – the empty space within transmembrane helices of HnSPNS calculated with HOLLOW [33] and represented as surface colored according to the charge it carries; left – a zoomed in view on the N-repeat face of central cavity; right – a zoomed in view on the C-repeat face of central cavity. The residues delineating the cavity were shown in ball-and-stick model with the conserved ones colored by elements. (b) A comparison among the central cavities found in solute transporter. The cavities coordinates were calculated on structures with PDB IDs 6e9c, 1pv6, 1pw4, and 4iu9, corresponding to hnSPNS, LacY, GlpT and NarU, respectively.

served in MFS proteins [27] was found at H2–H3 linker which interacts with H4 via hydrogen bond between D87 and S138 and with the "hinge loop" via a salt bridge between carboxyl oxygen of D87 and η-nitrogen of R233 (Fig. 3d). Further conserved residues interactions in this region include D142-G234 (H4-"hinge loop"), T141-R149 (H4–H5) and D87-S138 (H2–H4).

3.3. Putative substrate binding pocket

Neither prokaryotes nor eukaryotes have their SPNS substrate specificity being well characterized. The putative transported molecule includes sphingosine derivatives, carbohydrates, and lipids. The Fo-Fc map analysis on the native crystal structure of HnSPNS revealed significant and continuous electron density in the center of the transmembrane domain near to R42 and surrounded by almost all the conserved residues found in the inner cavity, suggesting the location of a putative substrate-binding site (Fig. 4). This unknown ligand density locates in the top space of the inner cavity of HnSPNS and has close contact with conserved basic residues R42 and R122, as well as aromatic residues F71, Y277, and Y371, which might serve to stabilize positive charges within membrane [29]. Among 25 residues surrounding the putative substrate density, 13 are highly hydrophobic amino acid and build a lipophilic pocket within the hydrophilic core of HnSPNS. Taken together, the HnSPNS structure proposes an acidic hydrophobic small molecule as carrying cargo and the evolutionary conservativeness in the binding pocket supports S1P as a potential substrate for eukaryotic SPNS. Since the said electron density was incomplete in the Fo-Fc map for structure solved using SeMet spinster protein as shown in Fig. S3 (online), the bound molecule might be enriched in LB medium for cell culture. To study the HnSPNS in "empty" state, the HnSPNS was further crystallized using protein purified from cells cultured in M9 minimal medium and the structure was solved without significant electron density in the inner cavity, supporting our speculation on the origination of the unknown ligand, while further efforts should be taken in seeking for alternative conformations in higher resolution since the possibility should not be excluded that the "empty" state might result from an artifact from relatively low-resolution crystallographic data (3.8 Å). The overall architectures for hnSPNS in substrate-bound and substrate-released states show very little difference and the RMSD between their main chains is calculated as 1.134 Å.

4. Discussion

Rocker-switch model is the most accepted theory in explaining the translocation process of solute through cell membrane and it involves a series global folding transitions among different conformations including outward-open (C_o), occluded/inward-open (C_i), as well as some partially open/occluded conformations as intermediate states [27,30], which could be represented by the structures of FucP (C_o) [26], XylE and EmrD (occluded) [31,32], LacY and GlpT (C_i) [24,25]. The HnSPNS structures represent two C_i conformations (occluded/inward open and empty) and the limited difference

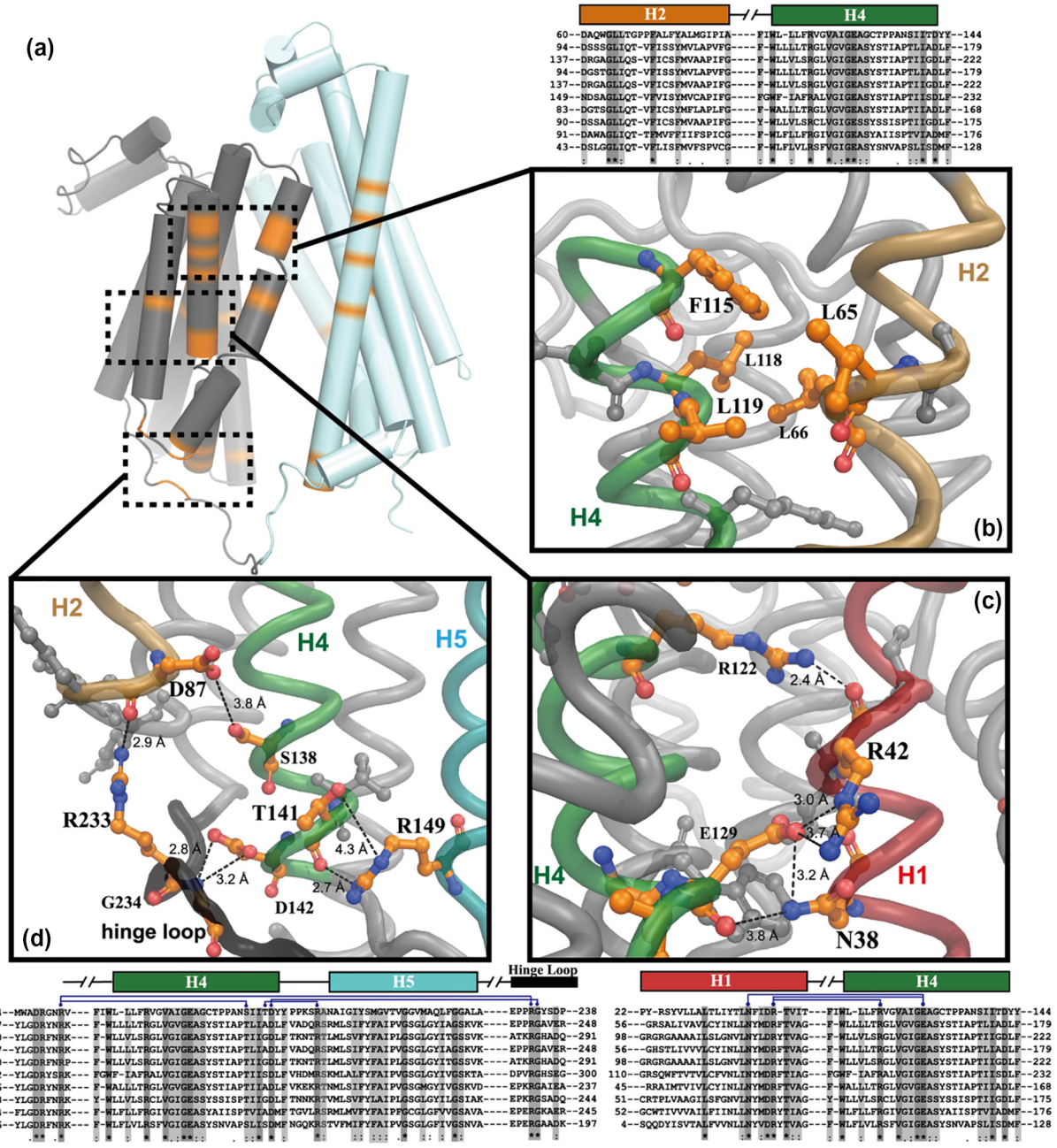

Fig. 3. The conserved loci in HnSPNS structure. (a) An overall view on the conserved residue within HnSPNS. The TM helices were shown as cylinder model with the N-repeat in gray and C-repeat in cyan color. The conserved residues within helices and loops were rendered in orange. The dashed frames indicate three conserved loci. (b–d) Close views on three conserved loci in HnSPNS Structure. The conserved residues were shown in ball-and-stick model and those participating the contacts were rendered by elements with others in gray. The dashed lines and the values in angstrom aside indicate the potential salt bridges formed form among helices and loop. The protein sequence alignments close to (b–d) show the residues conserved among HnSPNS, human spin-1, human spin-2, mouse spin-1, mouse spin-2, drosophila spinster, zebrafish spin-1, zebrafish spin-2, *C. elegans* spin-1 and spin-2 from top to bottom.

between them implies that the substrate release would not directly induce a switch process for spinster protein. Very little was known about the transportation mechanism of the spinster, our structures showed that a further event, such as an intracellular small molecular binding or protonation, was required for the spinster to switch back into its C_o conformation, which suggests that spinster might function as an antiporter, awaiting the evidences from further biochemical studies. Structural analysis on HnSPNS reveals an important role for H4 in the structural stability and conformation change. The fourth transmembrane helix of HnSPNS is comprised of amino acid 115–144, and 1/3 of residues are conserved among species from mammals, invertebrate, and bacteria, while 7 of them show highly strict conservation and keep unchanged in evolution. Those conserved in H4 closely interact with other conserved residues from H1, H2, H5 and hinge loop (Fig. 3d), via hydrophobic interaction, e.g., L66-L118, and salt bridges, e.g., E129-R42, implying a pivotal role of H4 during the conformation change caused by transporting activity. E129 induces a kink in the middle of H4 by the salt bridge form with R42 and thus might represent a switch for conformational change between C_i and C_o. As shown in

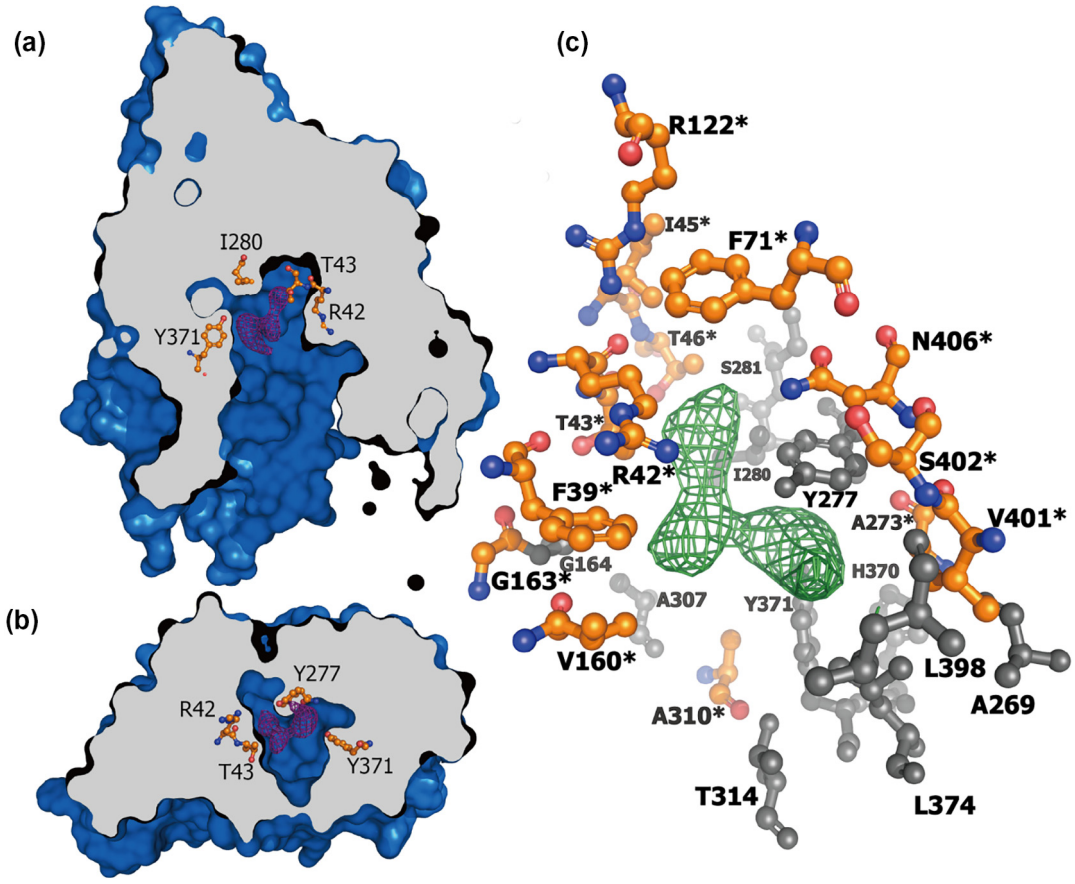

Fig. 4. The substrate binding pocket of HnSPNS. Cross-section views cut along the planes perpendicular (a) and parallel (b) to cell surface to show the putative binding pocket and the Fo-Fc electron density contoured at 2.5σ (in purple). (c) The residues closely interacting with the Fo-Fc electron density. The residues conserved among spinsters from various species are colored by elements and others in gray. The residues were labeled with single-letter amino acid abbreviation and the asterisks indicate conserved residues.

Fig. 5a, the protonation of E129 by cytosolic H^+ could break its ionic bonding with R42 and in turn relax the strain on H4 caused by the salt bridge, thereby inducing a series of re-arrangements among the helices closely interacted with H4 and driving the whole transporter into C_o conformation. A proposed transportation mechanism for spinster was shown in Fig. 5b.

Since HnSPNS inner cavity, especially the putative substrate-binding pocket, is delineated with high conserved residues, our HnSPNS structure could reveal useful information for the structure and function of eukaryotic spinsters. As a bacterial transporter, HnSPNS is believed to uptake energy molecules from environment into the cytosol to support its host growth, while the lysosomal spinster would conduct the influx or efflux of metabolites across lysosome membrane using the proton gradient across lysosomal membrane as an energy source, and the plasma membrane spinster mediates the release of S1P from cell. Compared with previously published MFS transporter structures, HnSPNS has an inner cavity with larger volume and, interestingly, much higher hydrophobicity (Fig. 2b), suggesting a big and oily substrate. Although the identity of the unknown ligand in HnSPNS is yet to be determined, the hydrophobic binding pocket with highly-conserved basic residues implies that spinster protein might transport acidic small molecules, e.g., phosphorylated hydrocarbon chain-containing molecules, such as S1P, or hydrophobic amino acids, which are abundant in lysosome from the hydrolysis reactions therein. Therefore, further structural and functional studies on the equivalent sites in eukaryotic spinster protein are needed for understanding the precise mechanism of spinster transportation.

Conflict of interest

The authors declare that they have no conflict of interest.

Acknowledgments

The authors thank Drs. Ming Zhou, Ming Lei and Lijun Wang for scientific discussion; Rijing Liao and Chao Peng for assistance with the data analysis. This work was supported by the National Key Research and Development Program of China (2017YFC1001303 and 2018YFC1004704), NSFC-CAS Joint Fund for Research Based on Large-Scale Scientific Facilities (U1632132), NSFC General Program (31670849) and SHIPM-pi fund (JY201804) from Shanghai Institute of Precision Medicine, Ninth People's Hospital Shanghai Jiao Tong University School of Medicine.

Author contributions

Y.C. and F.Z. initiated the study. Y.C., J.Z., and Y.Z. designed research and wrote the paper. F.Z. performed the purification and crystallization work. F.Z., R.B., L.Z., W.N., Y.C. and D.Y. collected and analyzed the data. D.Y. determined all the structure.

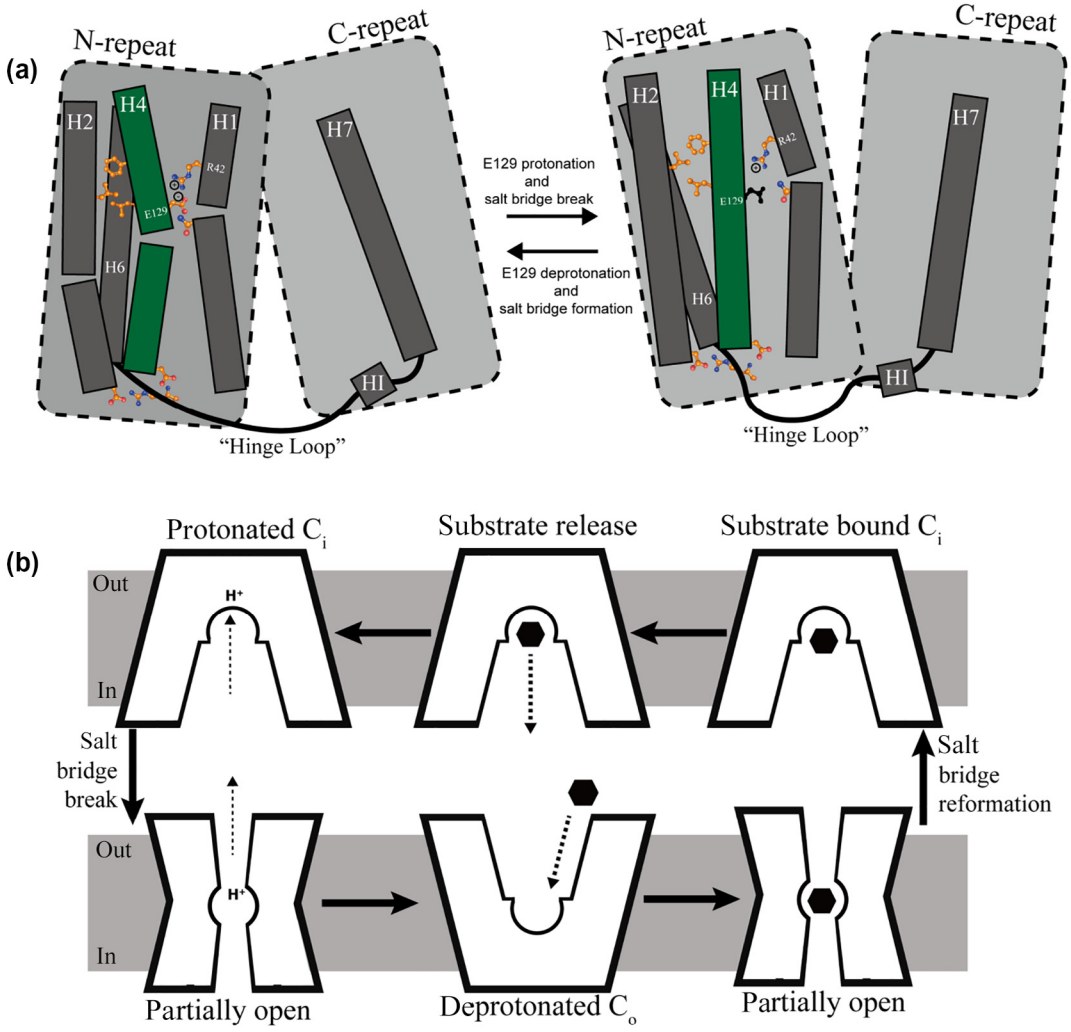

Fig. 5. (a) A proposed flip-over process driven by E129 protonation on H4 helices. Left: a cartoon representation based on the HnSPNS structure solved; Right: A putative model for the conformational change upon the protonation of E129 (residue in black). (b) A proposed model for substrate translocation mechanism of spinster. The substrate molecule is shown as solid hexagon and antiport co-substrate as solid triangle.

Data and materials availability

Shanghai Synchrotron Radiation Facility (SSRF) beamlines BL18U1 and BL19U1 are used for X-ray crystallography data collection. The coordinates are deposited at the PDB accession code: 6E8J, 6E9C and 6EBA.

Appendix A. Supplementary data

Supplementary data to this article can be found online at https://doi.org/10.1016/j.scib.2019.08.010.

References

[1] Dermaut B, Norga KK, Kania A, et al. Aberrant lysosomal carbohydrate storage accompanies endocytic defects and neurodegeneration in Drosophila benchwarmer. J Cell Biol 2005;170:127–39.
[2] Sweeney ST, Davis GW. Unrestricted synaptic growth in spinster-a late endosomal protein implicated in TGF-beta-mediated synaptic growth regulation. Neuron 2002;36:403–16.
[3] Nakano Y, Fujitani K, Kurihara J, et al. Mutations in the novel membrane protein spinster interfere with programmed cell death and cause neural degeneration in *Drosophila melanogaster*. Mol Cell Biol 2001;21:3775–88.
[4] Milton VJ, Jarrett HE, Gowers K, et al. Oxidative stress induces overgrowth of the Drosophila neuromuscular junction. Proc Natl Acad Sci USA 2011;108:17521–6.
[5] Yuva-Aydemir Y, Bauke AC, Klambt C. Spinster controls Dpp signaling during glial migration in the *Drosophila* eye. J Neurosci 2011;31:7005–15.
[6] Osborne N, Brand-Arzamendi K, Ober EA, et al. The spinster homolog, two of hearts, is required for sphingosine 1-phosphate signaling in zebrafish. Curr Biol 2008;18:1882–8.
[7] Balczerski B, Matsutani M, Castillo P, et al. Analysis of sphingosine-1-phosphate signaling mutants reveals endodermal requirements for the growth but not dorsoventral patterning of jaw skeletal precursors. Dev Biol 2012;362:230–41.
[8] van der Weyden L, Adams DJ. Genome-wide in vivo screen identifies novel host regulators of metastatic colonization. Nature 2017;541:233–6.
[9] Yanagisawa H, Ishii T, Endo K, et al. L-leucine and SPNS1 coordinately ameliorate dysfunction of autophagy in mouse and human Niemann-Pick type C disease. Sci Rep 2017;7:15944.
[10] Han M, Chang H, Zhang, et al. C13C4.5/spinster, an evolutionarily conserved protein that regulates fertility in C. elegans through a lysosome-mediated lipid metabolism process. Protein Cell 2013;4:364–72.
[11] Rong Y, McPhee CK, Deng S, et al. Spinster is required for autophagic lysosome reformation and mTOR reactivation following starvation. Proc Natl Acad Sci USA 2011;108:7826–31.
[12] Hebbar S, Khandelwal A, Jayashree R, et al. Lipid metabolic perturbation is an early-onset phenotype in adult spinster mutants: a *Drosophila* model for lysosomal storage disorders. Mol Biol Cell 2017;28:3728–40.
[13] Kawahara A, Nishi T, Hisano Y, et al. The sphingolipid transporter Spns2 functions in migration of zebrafish myocardial precursors. Science 2009;323:524–7.
[14] Fang V, Chaluvadi VS, Ramos-Perez WD, et al. Gradients of the signaling lipid S1P in lymph nodes position natural killer cells and regulate their interferon-gamma response. Nat Immunol 2017;18:15–25.
[15] Mendoza A, Fang V, Chen C, et al. Lymphatic endothelial S1P promotes mitochondrial function and survival in naive T cells. Nature 2017;546:158–61.

[16] Mendoza A, Bréart B, Ramos-Perez WD, et al. The transporter Spns2 is required for secretion of lymph but not plasma sphingosine-1-phosphate. Cell Rep 2012;2:1104–10.
[17] Tsai HC, Han MH. Sphingosine-1-phosphate (S1P) and S1P signaling pathway: therapeutic targets in autoimmunity and inflammation. Drugs 2016;76:1067–79.
[18] Kabsch W. Integration, scaling, space-group assignment and post-refinement. Xds. Acta Crystallogr D Biol Crystallogr 2010;66:125–32.
[19] Sheldrick GM. A short history of SHELX. Acta Crystallogr A 2008;64:112–22.
[20] Adams PD, Afonine PV, Bunkóczi G. PHENIX: a comprehensive Python-based system for macromolecular structure solution. Acta Crystallogr D Biol Crystallogr 2010;66:213–21.
[21] Murshudov GN, Skubák P, Lebedev AA, et al. REFMAC5 for the refinement of macromolecular crystal structures. Acta Crystallogr D Biol Crystallogr 2011;67:355–67.
[22] Winn MD, Ballard CC, Cowtan KD, et al. Overview of the CCP4 suite and current developments. Acta Crystallogr D Biol Crystallogr 2011;67:235–41.
[23] Emsley P, Cowtan K. Coot: model-building tools for molecular graphics. Acta Crystallogr D Biol Crystallogr 2004;60:2126–32.
[24] Huang Y, Lemieux MJ, Song J, et al. Structure and mechanism of the glycerol-3-phosphate transporter from Escherichia coli. Science 2003;301:616–20.
[25] Abramson J, Smirnova I, Kasho V, et al. Structure and mechanism of the lactose permease of *Escherichia coli*. Science 2003;301:610–5.
[26] Dang S, Sun L, Huang Y, et al. Structure of a fucose transporter in an outward-open conformation. Nature 2010;467:734–8.
[27] Law CJ, Maloney PC, Wang DN, et al. Ins and outs of major facilitator superfamily antiporters. Annu Rev Microbiol 2008;62:289–95.
[28] Voss NR, Gerstein M. 3V: cavity, channel and cleft volume calculator and extractor. Nucl Acids Res 2010;38:W555–62.
[29] Dougherty DA. Cation-pi interactions in chemistry and biology: a new view of benzene, Phe, Tyr, and Trp. Science 1996;271:163–8.
[30] Yan N. Structural advances for the major facilitator superfamily (MFS) transporters. Trends Biochem Sci 2013;38:151–9.
[31] Yin Y, He X, Szewczyk P, et al. Structure of the multidrug transporter EmrD from *Escherichia coli*. Science 2006;312:741–4.
[32] Sun L et al. Crystal structure of a bacterial homologue of glucose transporters GLUT1-4. Nature 2012;490:361–6.
[33] Ho BK, Gruswitz F. HOLLOW: generating accurate representations of channel and interior surfaces in molecular structures. BMC Struct Biol 2008;8:49.

Fu Zhou is a senior Ph.D. candidate at University of Chinese Academy of Sciences and Institute of Biochemistry and Cell Biology, Chinese Academy of Sciences. His research focuses on the metabolites transportation among the cell organelles.

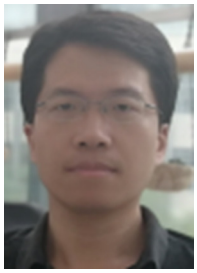

Deqiang Yao is a Research Associate Professor at iHuman Institute, ShanghaiTech University. He received his Ph.D. degree from University of Science and Technology of China and conducted postdoctoral research at *Institut Pasteur* in Paris, France and McGill University in Montreal, Canada. Dr. Yao's major research interest is macromolecular crystallography.

Jie Zhao is a Professor and the Chairman of Orthopaedic Department in Shanghai Ninth People's Hospital, Shanghai Jiao Tong University School of Medicine. Dr. Zhao received his Ph.D. degree from Shanghai Second Military Medical University. His research interest focuses on the organelle dysfunction in skeletal dysplasia.

Yu Cao is a Principal Investigator at Shanghai Institute of Precision Medicine and Adjunct Professor in Orthopaedic Department, Shanghai Ninth People's Hospital, Shanghai Jiao Tong University School of Medicine. He received Ph.D. degree in the Institute of Biophysics, Chinese Academy of Sciences and conducted postdoctoral research in Columbia University at New York, USA and Pfizer Inc. His research interest focuses on transmembrane biological process and the molecular pathology.